MJFAS MALAYSIAN JOURNAL OF FUNDAMENTAL AND APPLIED SCIENCES
PRINT ISSN: 2289-5981 | ONLINE ISSN: 2289-599X

RESEARCH ARTICLE

Heat generation effect on mixed convection flow of viscoelastic nanofluid: convective boundary condition solution

Rahimah Mahat [a, b], Noraihan Afiqah Rawi [b], Abdul Rahman Mohd Kasim [c], Sharidan Shafie [b,*]

[a] *Technical Foundation, Universiti Kuala Lumpur Malaysian Institute of Industrial Technology Malaysia, Persiaran Sinaran Ilmu, 81750 Johor Bahru, Johor*
[b] *Department of Mathematics, Faculty of Science, Universiti Teknologi Malaysia, 81310 UTM Johor Bahru, Johor, Malaysia*
[c] *Universiti Malaysia Pahang, Lebuhraya Tun Razak, 26300, Gambang Kuantan, Pahang*

* *Corresponding author: sharidan@utm.edu.my*

Article history
Received 19 December 2018
Revised 6 Mac 2019
Accepted 25 November 2019
Published Online 15 April 2020

Abstract

The steady two-dimensional mixed convection boundary layer flow of viscoelastic nanofluid past a circular cylinder by considering convective boundary condition with heat generation has been studied numerically. For the case of nanofluid, the base fluid chosen is Carboxymethyl cellulose solution (CMC) and the nanoparticle is copper. The Tiwari-Das model has been considered in this study. Similarity transformation has been introduced by reducing the governing partial differential equations to a system of ordinary differential equations. Then, the Keller-box is applied to solve the nonlinear similarity. The numerical results are presented graphically and analytically for different values of the parameters including the heat generation parameter, nanoparticles volume fraction, and Biot number. A systematic study is discussed to analyze the effect of these parameters on the velocity and temperature profiles, as well as the skin friction and heat transfer coefficient. The thermal boundary layer shows the changes in variation behavior when the nanoparticles volume fraction, heat generation, and Biot number are increased. Heat transfer coefficient is an increasing function of heat generation parameter. Nanoparticles volume fraction on heat transfer coefficient has the opposite effect when compared with the heat generation parameter.

Keywords: Mixed convection, viscoelastic, nanofluid, convective boundary condition, heat generation

INTRODUCTION

Nanotechnology has been long-established in many industrial and engineering applications because high thermal conductivity. The term nanofluid was first used by Choi (1995), which refers to a base liquid with suspended solid nanoparticles. Fluid flows past a horizontal circular cylinder are beneficial to many engineering and several industrial-manufacturing processes involving petroleum drilling, manufacturing of foods, and paper. Studies on the mixed convection flow past a cylinder have been carried out by numerous researchers, pioneered by Merkin (1977) where studied the mixed convection from a horizontal circular cylinder. This problem was then extended by Nazar *et al*. (2004) to include the constant surface heat flux in the Newtonian problem considered in both works. Later, Anwar *et al*. (2008) considered a non-Newtonian problem which is viscoelastic fluid.

Salleh *et al.* presented (2010) numerical solutions of the same problem of Nazar *et al*. (2004) but with different boundary condition which is Newtonian heating. The recent issues of mixed convection past a horizontal circular cylinder were carried out by Tham *et al*. (2016), Sulochana and Sandeep (2016), and Mahat *et al*. (2017, 2018). Since nanofluid has a higher thermal conductivity compared to usual liquids, the fluid has high potential to enhance heat transfer rate in engineering systems especially for cooling of electronic devices (Kasaeian *et al*., 2017), thermal energy storage, and filtering devices (Raju *et al*., 2014).

On the other hand, the study of heat generation in moving fluids is important in problems dealing with chemical reactions and those concerned with dissociating fluids. Possible heat generation effects may alter the temperature distribution and consequently, the particle deposition rate in nuclear reactors, electronic chip sand semi-conductor wafers (Chamkha and Ahmed, 2011). A number of physical phenomena also involve convection that is driven by heat generation. Vajravelu and Hadjinicolaou (1993) were the first individuals who explored the effect of heat generation and viscous dissipation over a linearly stretching continuous surface in a viscous fluid. Chamkha (2002) analyzed numerically on hydromagnetic-combined convection flow in a vertical lid-driven cavity with internal heat generation or absorption. Again, Chamkha *et al.* (2006) considered the problem of the thermophoretic free convection boundary layer from a vertical flat plate embedded in a porous medium with the presence of heat generation or absorption. On the same year, Hady *et al*. (2006) studied MHD free convection flow along a vertical wavy surface with heat generation or absorption effect. A comprehensive analysis of conjugate heat transfer for a vertical flat plate with heat generation effect has been provided by Mamun *et al*. (2008).

Later on, Kasim *et al*. (2011) have considered the topic on free convection flow with heat generation in viscoelastic fluid with the same

geometry, which is a circular cylinder. From the investigation, they found that the parameter heat generation is significant on shear stress and velocity and temperature profile. Other extensions of Kasim *et al*. (2012) has considered the constant surface heat flux as a boundary condition. Both problems were solved by using the Keller-box method. Contrarily, the implicit finite difference Crank-Nicolson method for the Newtonian problem on a horizontal circular cylinder in the presence of heat generation and radiation were presented by Zainuddin *et al*. (2014, 2015). Olanrewaju *et al*. (2012) considered the internal heat generation effect on thermal boundary layer with a convective surface boundary condition and the problems were solved numerically by applying shooting iteration technique together with a fourth order Runge-Kutta integration scheme.

The analytic and numeric solutions of heat generation/absorption effects in a boundary layer stretched flow of maxwell nanofluid has been presented by Awais *et al*. (2015). Authors have employed shooting method for numerical approach which utilizes the Runge-Kutta-4 (RK4) and secant method whereas homotopy analysis method (HAM) is for the analytic approach. Later, Reddy and Chamkha (2016) investigated the soret and dufour effects past a stretching sheet in porous media with heat generation/absorption in the presence of aluminium oxide (Al_2O_3–water) and titanium oxide (TiO_2–water) nanofluid. We have considered copper-water as a base nanofluid in this problem because copper has the highest factor for heat transfer enhancement as reported by Nazar *et al.* (2011). Rashad *et al*. (2017) conducted the numerical study of magnetic field and internal heat generation effects on the free convection in a rectangular cavity filled with a porous medium saturated with copper–water nanofluid. They have utilized the finite difference method to analyze the outcomes of the problem.

Other than the aforementioned steady cases, there were also researches on unsteady cases. Chamkha and Al-Mudhaf (2005) have considered the unsteady heat and mass transfer from a rotating vertical cone with a magnetic field and heat generation or absorption effects. Then, Chamkha and Ahmed (2011) obtained a similarity solution of unsteady magnetohydrodynamics (MHD) flow near a stagnation point of a three-dimensional porous body with heat and mass transfer, heat generation/absorption, and chemical reaction. Khan *et al*. (2014) presented the effects of heat generation on unsteady mixed convection flow from a vertical porous plate with induced magnetic field. Ullah *et al*. (2016) recently presented the unsteady MHD mixed convection slip flow of casson fluid over nonlinearly stretching sheet embedded in a porous medium with chemical reaction, thermal radiation, heat generation/absorption, and convective boundary conditions.

Interestingly, this paper aims to study the effect of heat generation on steady mixed convection boundary layer flow of viscoelastic nanofluid past a horizontal circular cylinder by considering the convective boundary condition. To the best knowledge of the authors, there is no study yet to be reported in the literature. The thermal performance on flow and heat transfer characteristics are investigated.

MATHEMATICAL FORMULATION

The steady mixed convection boundary layer flow past a horizontal circular cylinder of radius a placed in a viscoelastic nanofluid with convective boundary condition and heat generation is considered. It is assumed that the velocity outside the boundary is $\bar{u}_e(\bar{x})$ and the temperature of the ambient nanofluid is T_∞, while the temperature of the surface of the cylinder is $-k\dfrac{\partial T}{\partial \bar{y}} = h_f\left(T_f - T\right)$ as shown in Fig. 1.

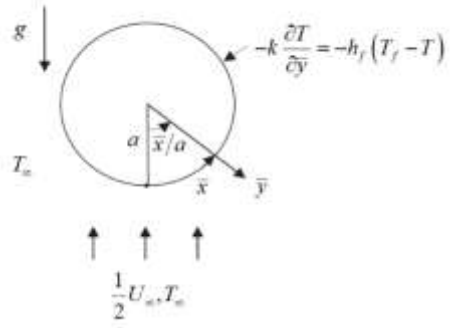

Fig. 1 Coordinates system and the flow model.

By above assumptions and using the model of the nanofluid proposed by Tiwari and Das (2007), the equations governing this problem are as follows, see also Merkin (1977), Kasim *et al*. (2012):

$$\frac{\partial \bar{u}}{\partial \bar{x}} + \frac{\partial \bar{v}}{\partial \bar{y}} = 0, \tag{1}$$

$$\rho_{nf}\left(\bar{u}\frac{\partial \bar{u}}{\partial \bar{x}} + \bar{v}\frac{\partial \bar{u}}{\partial \bar{y}}\right) = \rho_{nf}\bar{u}_e\frac{\partial \bar{u}_e}{\partial \bar{x}} + \mu_{nf}\frac{\partial^2 \bar{u}}{\partial \bar{y}^2} + k_0\left[\frac{\partial}{\partial \bar{x}}\left(\bar{u}\frac{\partial^2 \bar{u}}{\partial \bar{y}^2}\right) + \bar{v}\frac{\partial^3 \bar{u}}{\partial \bar{y}^3} - \frac{\partial \bar{u}}{\partial \bar{y}}\frac{\partial^2 \bar{u}}{\partial \bar{x}\partial \bar{y}}\right] + g\left(\rho\beta\right)_{nf}\left(T - T_\infty\right)\sin\left(\frac{\bar{x}}{a}\right), \tag{2}$$

$$\bar{u}\frac{\partial T}{\partial \bar{x}} + \bar{v}\frac{\partial T}{\partial \bar{y}} = \alpha_{nf}\frac{\partial^2 T}{\partial \bar{y}^2} + \frac{Q_o}{\left(\rho C_p\right)_{nf}}\left(T - T_\infty\right) \tag{3}$$

subjected to boundary conditions

$$\bar{u} = 0, \quad \bar{v} = 0, \quad -k\frac{\partial T}{\partial \bar{y}} = h_f\left(T_f - T\right) \quad \text{at} \quad \bar{y} = 0, \ \bar{x} \geq 0,$$
$$\bar{u} = \bar{u}_e(\bar{x}), \quad \frac{\partial \bar{u}}{\partial \bar{y}} = 0, \quad T = T_\infty \quad \text{as} \quad \bar{y} \to \infty, \ \bar{x} \geq 0, \tag{4}$$

where

$$\mu_{nf} = \frac{\mu_f}{(1-\phi)^{2.5}}, \quad \rho_{nf} = (1-\phi)\rho_f + \phi\rho_s,$$
$$\left(\rho C_p\right)_{nf} = (1-\phi)\left(\rho C_p\right)_f + \phi\left(\rho C_p\right)_s,$$
$$\alpha_{nf} = \frac{k_{nf}}{\left(\rho C_p\right)_{nf}}, \quad k_{nf} = k_f\frac{\left(k_s + 2k_f\right) - 2\phi\left(k_f - k_s\right)}{\left(k_s + 2k_f\right) + \phi\left(k_f - k_s\right)}. \tag{5}$$

Here $\bar{x}$ and $\bar{y}$ are the Cartesian coordinates along the surface of the cylinder. Besides, $\bar{y}$ is the coordinate measured normal to the surface of the cylinder, $\bar{u}$ and $\bar{v}$ are the velocity components, g is the gravity acceleration, T is the temperature of selected fluid, $k_0 > 0$ is the constant of the viscoelastic material (Walter's Liquid-B model), Q_o is the heat generation constant, ϕ is the nanoparticle volume fraction, $(\beta)_{nf}$ is the coefficient of thermal expansion of nanofluid, $\left(\rho C_p\right)_{nf}$ is the heat capacitance of nanofluid, k_{nf} is the thermal conductivity of

the nanofluid, k_f and k_s are the thermal conductivities of the fluid and of the solid fractions, respectively, ρ_{nf} and μ_{nf} are the density and dynamic viscosity of nanofluid, μ_f is the viscosity of the fluid fraction, and α_{nf} is the thermal diffusivity of the nanofluid. The thermophysical properties of the base fluid (CMC-water) and nanoparticles are given in Table 1 (Lin *et al*. (2014)).

Table 3 Thermophysical properties of nanoparticles and base fluid.

Physical Properties	$\rho\left(\text{kg m}^{-3}\right)$	$C_p\left(\text{J kg}^{-1}\text{K}^{-1}\right)$	$k\left(\text{Wm}^{-1}\text{K}^{-1}\right)$	$\beta\times10^5\left(\text{K}^{-1}\right)$
Based fluid	997.1	4179	0.613	21
Nanoparticle (Cu)	8933	385	401	1.67

Following Merkin (1977) and Nazar *et al*. (2002), we introduce the dimensionless variables defined as

$$x=\bar{x}/a,\ y=\text{Re}^{1/2}\left(\bar{y}/a\right),\ u=\bar{u}/U_\infty,\ v=\text{Re}^{1/2}\left(\bar{v}/U_\infty\right),\\ u_e\left(x\right)=\bar{u}_e\left(\bar{x}\right)/U_\infty,\ \theta=\left(T-T_\infty\right)/\left(T_f-T_\infty\right), \tag{6}$$

where $\text{Re}=U_\infty a/\nu$ is the Reynolds number. Substitution of equation (5) into equations (1) to (3) leads to the following dimensionless equations:

$$\frac{\partial u}{\partial x}+\frac{\partial v}{\partial y}=0, \tag{7}$$

$$\left[\left(1-\phi\right)+\phi\frac{\rho_s}{\rho_f}\right]\left[u\frac{\partial u}{\partial x}+v\frac{\partial u}{\partial y}\right]=\left[\left(1-\phi\right)+\phi\frac{\rho_s}{\rho_f}\right]u_e\frac{\partial u_e}{\partial x}\\ +\frac{1}{\left(1+\phi\right)^{2.5}}\frac{\partial^2 u}{\partial y^2}+K\left[\frac{\partial}{\partial x}\left(u\frac{\partial^2 u}{\partial y^2}\right)+v\frac{\partial^3 u}{\partial y^3}-\frac{\partial u}{\partial y}\frac{\partial^2 u}{\partial x\partial y}\right]\\ +\left[\left(1-\phi\right)+\phi\frac{\left(\rho\beta\right)_s}{\left(\rho\beta\right)_f}\right]\lambda\theta\sin\left(x\right), \tag{8}$$

$$\left[\left(1-\phi\right)+\phi\frac{\left(\rho C_p\right)_s}{\left(\rho C_p\right)_f}\right]\left[u\frac{\partial\theta}{\partial x}+v\frac{\partial\theta}{\partial y}\right]\\ =\frac{\left(k_s+2k_f\right)-2\phi\left(k_f-k_s\right)}{\left(k_s+2k_f\right)+\phi\left(k_f-k_s\right)}\frac{1}{\text{Pr}}\frac{\partial^2\theta}{\partial y^2}+\gamma_2\theta \tag{9}$$

and the boundary conditions (4) become

$$u=0,\quad v=0,\quad \frac{\partial\theta}{\partial y}=-\gamma_1\left(1-\theta\right)\ \text{at}\ \ y=0,\ x\geq0,\\ u=u_e\left(x\right),\quad \frac{\partial u}{\partial y}=0,\quad \theta=0\quad \text{as}\ \ y\to\infty,\ x\geq0, \tag{10}$$

where $\gamma_2=Q_o a/\left(\rho C_p\right)_f U_\infty$ is the heat generation parameter, $\text{Pr}=\upsilon/\alpha$ is the Prandtl number, $K=k_0U_\infty/a\rho\upsilon$ is the dimensionless viscoelastic parameter, γ_1 is the Biot number, and $\lambda=Gr/\text{Re}^2$ is the constant mixed convection parameter, where $Gr=g\beta\left(T_w-T_\infty\right)a^3/\nu^2$ is known as a Grashof number. It should be declared that the assisting flow (heated cylinder) is when $\lambda>0$, the opposing flow (cooled cylinder) is when $\lambda<0$ and the forced convection flow is when $\lambda=0$. It should also be mentioned that for the case of viscous (Newtonian) fluids, $K=0$.

Solution

The following variables were assumed in order to solve equations (7)–(9), together with the boundary conditions (10)

$$\psi=xF(x,y),\qquad \theta=\theta(x,y), \tag{11}$$

where ψ, the stream function is defined as

$$u=\frac{\partial\psi}{\partial y},\qquad v=-\frac{\partial\psi}{\partial x}, \tag{12}$$

that automatically satisfy equation (7). By substituting equation (12) to (8)–(10), and considering that $u_e\left(x\right)=\sin x$, we obtain

$$\left[\left(1-\phi\right)+\phi\frac{\rho_s}{\rho_f}\right]\left[\left(\frac{\partial F}{\partial y}\right)^2+x\frac{\partial F}{\partial y}\left(\frac{\partial^2 F}{\partial x\partial y}\right)-x\frac{\partial F}{\partial x}\frac{\partial^2 F}{\partial y^2}-F\frac{\partial^2 F}{\partial y^2}\right]\\ =\left[\left(1-\phi\right)+\phi\frac{\rho_s}{\rho_f}\right]\frac{\sin x\cos x}{x}+\frac{1}{\left(1+\phi\right)^{2.5}}\frac{\partial^3 F}{\partial y^3}\\ +\left[\left(1-\phi\right)+\phi\frac{\left(\rho\beta\right)_s}{\left(\rho\beta\right)_f}\right]\lambda\theta\frac{\sin x}{x}+K\left[\begin{array}{l}2\dfrac{\partial F}{\partial y}\dfrac{\partial^3 F}{\partial y^3}-F\dfrac{\partial^4 F}{\partial y^4}-\left(\dfrac{\partial^2 F}{\partial y^2}\right)^2\\ +x\left(\dfrac{\partial^2 F}{\partial x\partial y}\dfrac{\partial^3 F}{\partial y^3}-\dfrac{\partial F}{\partial x}\dfrac{\partial^4 F}{\partial y^4}\right.\\ \left.+\dfrac{\partial F}{\partial y}\dfrac{\partial^4 F}{\partial x\partial y^3}-\dfrac{\partial^2 F}{\partial y^2}\dfrac{\partial^3 F}{\partial x\partial y^2}\right)\end{array}\right], \tag{13}$$

$$\frac{\left(k_s+2k_f\right)-2\phi\left(k_f-k_s\right)}{\left(k_s+2k_f\right)+\phi\left(k_f-k_s\right)}\frac{1}{\text{Pr}}\frac{\partial^2\theta}{\partial y^2}+\gamma_2\theta\\ -\left[\left(1-\phi\right)+\phi\frac{\left(\rho C_p\right)_s}{\left(\rho C_p\right)_f}\right]x\frac{\partial F}{\partial y}\frac{\partial\theta}{\partial x}+\left[\left(1-\phi\right)+\phi\frac{\left(\rho C_p\right)_s}{\left(\rho C_p\right)_f}\right]x\frac{\partial F}{\partial x}\frac{\partial\theta}{\partial y}\\ +\left[\left(1-\phi\right)+\phi\frac{\left(\rho C_p\right)_s}{\left(\rho C_p\right)_f}\right]F\frac{\partial\theta}{\partial y}=0 \tag{14}$$

along with the boundary conditions

$$F=0,\quad \frac{\partial F}{\partial y}=0,\quad \frac{\partial\theta}{\partial y}=-\gamma_1\left(1-\theta\right),\ \text{at}\ y=0,\ x\geq0,\\ \frac{\partial F}{\partial y}=\frac{\sin x}{x},\quad \frac{\partial^2 F}{\partial y^2}=0,\quad \theta=0,\qquad \text{as}\ y\to\infty,\ x\geq0. \tag{15}$$

At the lower stagnation point of the cylinder, $x\approx0$, equations (13) and (14) reduce to the following ordinary differential equations

$$\frac{1}{\left(1+\phi\right)^{2.5}}f'''-\left[\left(1-\phi\right)+\phi\frac{\rho_s}{\rho_f}\right]\left[f'^2-ff''\right]\\ +K\left(2ff'''-ff^{iv}-f'^2\right)+\left[\left(1-\phi\right)+\phi\frac{\left(\rho\beta\right)_s}{\left(\rho\beta\right)_f}\right]\lambda\theta=0, \tag{16}$$

$$\frac{\left(k_s+2k_f\right)-2\phi\left(k_f-k_s\right)}{\left(k_s+2k_f\right)+\phi\left(k_f-k_s\right)}\frac{1}{\text{Pr}}\theta''+\gamma_2\theta\\ +\left[\left(1-\phi\right)+\phi\frac{\left(\rho C_p\right)_s}{\left(\rho C_p\right)_f}\right]f\theta'=0 \tag{17}$$

and the boundary conditions (15) become

$$f(0)=0,\quad f'(0)=0,\quad \theta'(0)=-\gamma_1\left(1-\theta(0)\right),$$
$$f'(\infty)=1,\quad f''(\infty)=0,\quad \theta(\infty)=0, \tag{18}$$

where primes express differentiation with respect to η. For a Newtonian fluid $(K=0)$, equations (13) and (14) and equations (16) and (17) reduce to the case investigated by Nazar *et al*. (2004). The physical quantities of principal interest in this problem are the skin friction coefficient C_f and heat transfer coefficient $\theta_w(x)$. We define these coefficients in non-dimensional form as

$$C_f=\mathrm{Re}^{1/2}\frac{\tau_w}{\rho U_\infty^2},\ \theta_w(x)=\mathrm{Re}^{-1/2}\frac{aq_w}{k\left(T_w-T_\infty\right)}, \tag{19}$$

where *k* being the thermal conductivity of the viscoelastic fluid. The surface shear stress or skin friction and the surface heat flux are given by

$$\tau_w=\mu_{nf}\left(\frac{\partial\bar{u}}{\partial\bar{y}}\right)_{\bar{y}=0}+k_0\left(\bar{u}\frac{\partial^2\bar{u}}{\partial\bar{x}\partial\bar{y}}+\bar{v}\frac{\partial^2\bar{u}}{\partial\bar{y}^2}+2\frac{\partial\bar{u}}{\partial\bar{x}}\frac{\partial\bar{u}}{\partial\bar{y}}\right)_{\bar{y}=0},$$
$$q_w=-k_{nf}\left(\frac{\partial T}{\partial\bar{y}}\right)_{y=0}. \tag{20}$$

Using (6) and (12), we obtain

$$C_f(x)=\frac{1}{(1-\phi)^{2.5}}x\left(\frac{\partial^2F}{\partial y^2}\right)_{\bar{y}=0},$$
$$\theta_w(x)=-\frac{k_{nf}}{k_f}\left(\frac{\partial\theta}{\partial y}\right)_{\bar{y}=0}. \tag{21}$$

RESULTS AND DISCUSSION

CMC-water-based nanofluid with nanoparticles of Cu were used in this research to examine the transport phenomena past a horizontal circular cylinder with convective boundary condition in presence of heat generation. The systems of equations (13)–(14) and (16)–(17) were solved numerically for some values of Biot number γ_1, heat generation parameter γ_2, and nanoparticles volume fraction ϕ. The values used for all the physical parameters were referring from the previous validated literature. The accuracy and robustness of Keller-box method used have been repeatedly confirmed in the previous publication Nazar *et al*. (2002) in Fig. 2 in the case of constant wall temperature $(\gamma\to\infty)$. The constant temperature results were recovered by using a value of $\gamma\to\infty$ in the third boundary condition in equation (18) in this study which then gives the condition $\theta'(0)=1$ (isothermal condition). The results of Fig. 2 manifest a trend similar to that found in mixed convection flow past a horizontal circular cylinder in a regular fluid where the heat transfer increases with the increase in the mixed convection parameter λ. Thus, this supports the validity of present graphical results for dimensionless velocity, temperature, skin friction, and heat transfer coefficients rate.

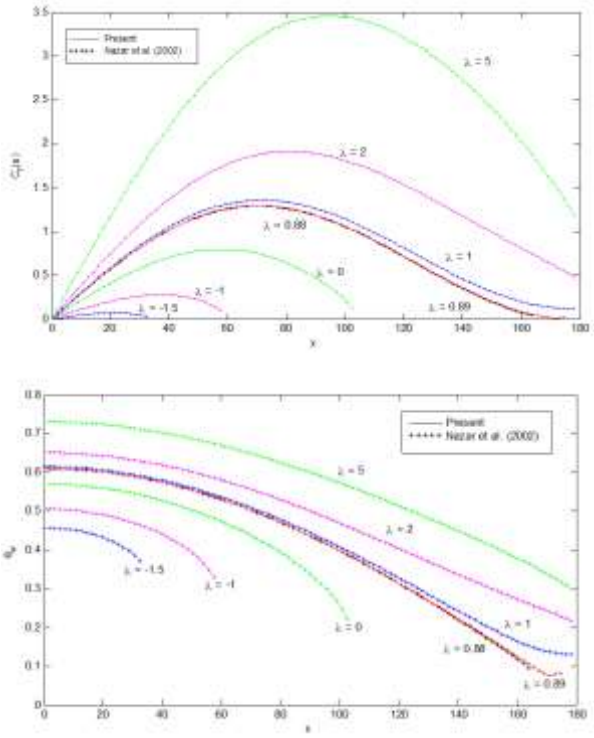

Fig. 2 Comparison of results for different values of mixed convection parameter λ.

Fig. 3 to Fig. 5 exhibit the dimensionless velocity and temperature profiles for various values of the flow-controlling parameters, namely Biot number γ_1, heat generation parameter γ_2, and nanoparticles volume fraction ϕ. Fig. 3 illustrates the effect of Biot number on the velocity and temperature distributions in the momentum and thermal boundary layer, respectively, for the case of assisting flow. In the figure, both velocity $f'(\eta)$ and temperature $\theta(\eta)$ increases as the parameter γ_1 is increased. While $\gamma_1\to\infty$, the solution approaches the classical solution for the constant surface temperature where the boundary condition (18) reduces to $\theta(0)=1$, as illustrated in Fig. 3. As expected, the stronger convection results in higher surface temperatures, causing the thermal effect to penetrate deeper into the fluid.

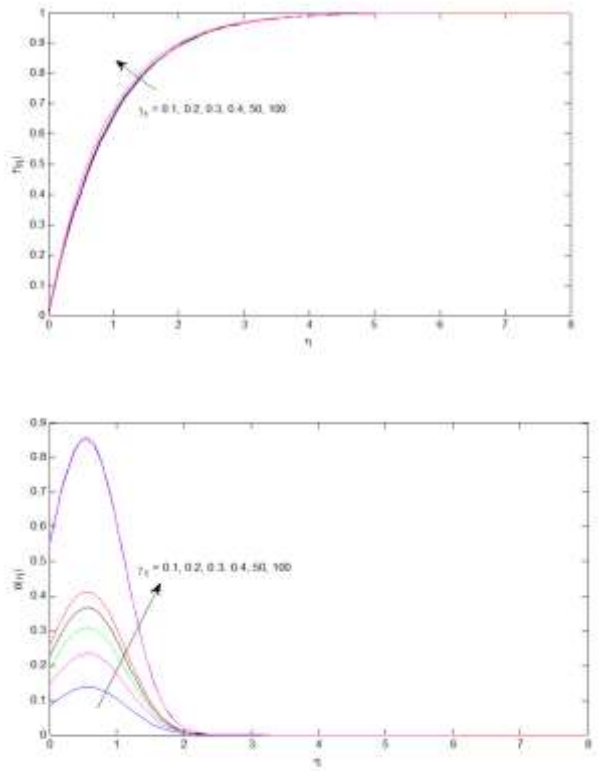

Fig. 3 Velocity and temperature profiles for different values of Biot number γ_1 when $K=1,\ \lambda=1,\ \phi=0.1,\ \gamma_2=0.2$.

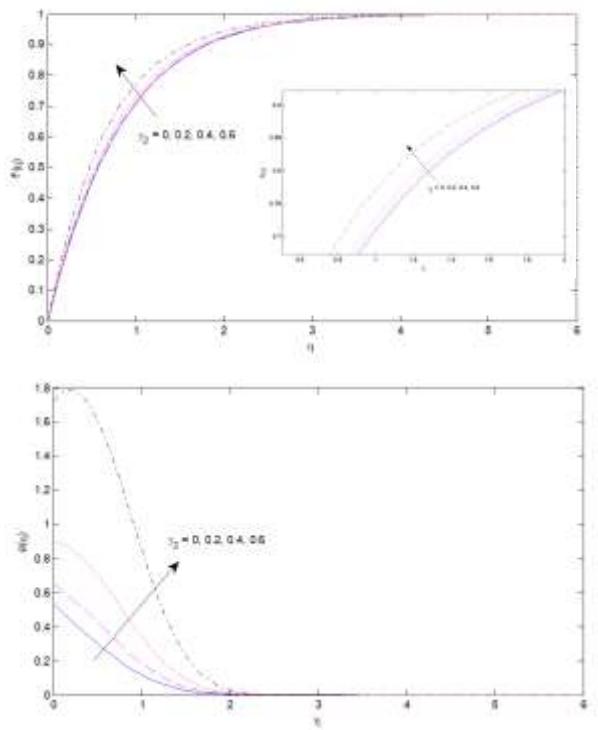

Fig. 4 Effect of heat generation profiles when $K=1,\ \lambda=1,\ \gamma_1=0.2,\ \phi=0.1$ velocity and temperature

.

Fig. 4 illustrates the velocity and temperature distributions against η, for different values of heat generation parameter, $\gamma_2=0,0.2,0.4,0.6$. Fig. 4 illustrates the velocity and temperature distributions at stagnation point against different values of the heat generation parameter γ_2, with constant values of Prandtl number, $\Pr=6.2$, and viscoelastic parameter, $K=1$. From the observation, the velocity and temperature distribution show an increment with the increase in the value of heat generation parameter. In the meantime, from the temperature profiles, it is seen that with the effect of heat generation, the temperature distribution increases pronouncedly. Fig. 5 presents the effect of nanoparticles volume fraction ϕ on velocity profile and temperature distribution. From the figure, it can be seen that the velocity distribution shows an increment with the increase in the value of nanoparticles volume fraction. While the temperature distribution decreased near the surface, at one point it increased significantly until asymptotically fulfil the boundary condition.

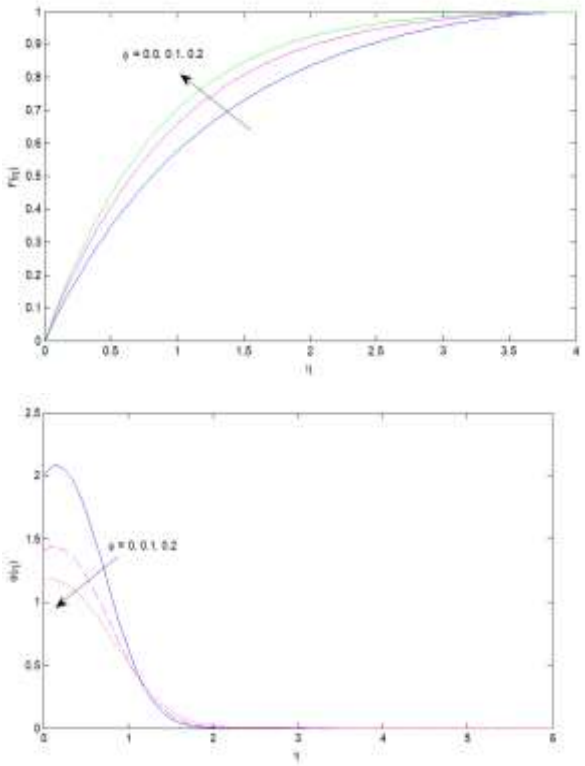

Fig. 5 Effect of nanoparticles volume fraction ϕ on velocity and temperature profiles when $K=1,\ \lambda=1,\ \gamma_1=0.2,\ \gamma_2=0.2$.

Fig. 6 and Fig. 7 predict the effects of nanoparticles volume fraction ϕ and heat generation parameter γ_2 on the skin friction and heat transfer coefficients, respectively. For Fig. 6, it is seen that the heat transfer coefficient decreases while skin friction coefficient increases when ϕ increases which is in agreement with the results reported by Sheikholeslami *et al*. (2012). On the other hand, for Fig.7, it is found that an increase in heat generation parameter, γ_2 leads to an increase in both the skin friction and heat transfer coefficients. These are expected, since the heat generation mechanism creates a layer of hot fluid near the surface.

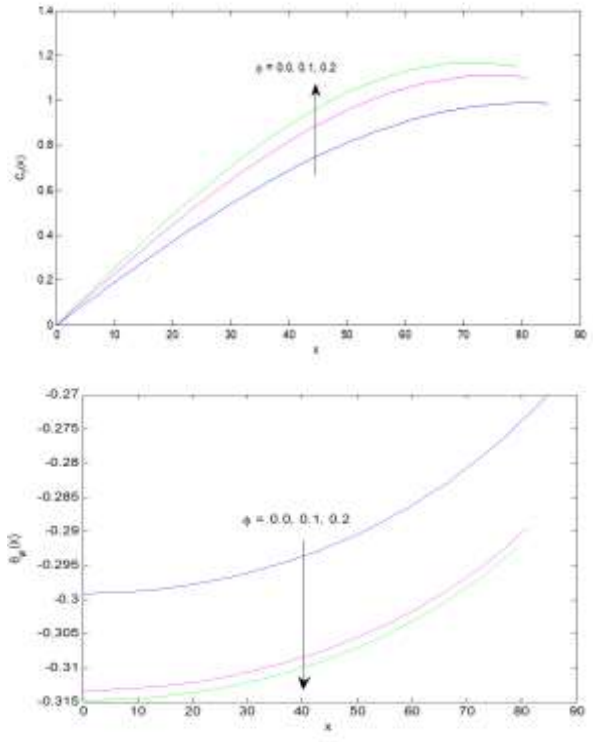

Fig. 6 Effect of nanoparticles volume fraction ϕ on skin friction and heat transfer coefficient when $K=1,\ \lambda=1,\ \gamma_1=0.2,\ \gamma_2=0.2$.

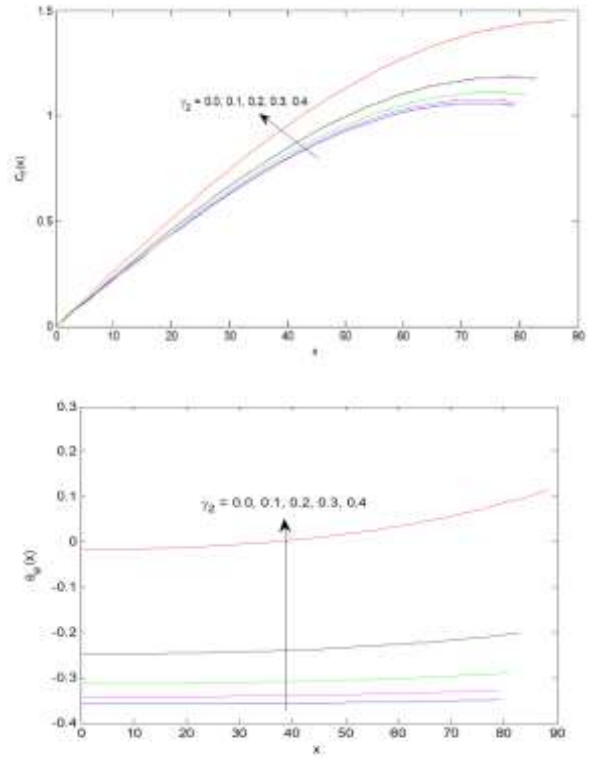

Fig. 7 Effect of heat generation γ_2 on skin friction and heat transfer coefficients when $K=1,\ \lambda=1,\ \gamma_1=0.2,\ \phi=0.1$.

CONCLUSION

Numerical analysis for the steady mixed convection boundary layer flow past a horizontal circular cylinder subject to a convective boundary condition and heat generation has been examined theoretically and graphically. The following conclusions are drawn based on the present investigation:

- The skin-friction and heat transfer coefficients increase when the value γ_2 increases.
- An increase in the values of γ_2 leads to an increase in both the velocity and temperature distribution. As γ_2 increases, the velocity and thermal boundary layer thickness increased.
- Both velocity and temperature profiles increase as the parameter γ_1 is increased.
- The velocity boundary layer decreases while the temperature profiles are characterized by distinctive peaks in the immediate vicinity of the wall, and as ϕ increases these peaks decrease and move gradually downstream.
- The heat transfer coefficient decreases while skin friction coefficient increases when ϕ increases.

ACKNOWLEDGEMENT

The authors would like to acknowledge the Center for Research and Innovation, UniKL; Research Management Centre, UTM; and Ministry of Higher Education (MOHE), Malaysia for the financial support through vote numbers STRG 15095, 13H74, and 4F713 for this research.

REFERENCES

Anwar, I., N. Amin, I. Pop. 2008. Mixed convection boundary layer flow of a viscoelastic fluid over a horizontal circular cylinder. *International Journal of Non-Linear Mechanics* 43(9): 814–821.

Awais, M., T. Hayat, S. Irum, A. Alsaedi. 2015. Heat Generation/absorption effects in a boundary layer stretched flow of maxwell nanofluid: Analytic and numeric solutions. *PLoS ONE* 10(6): 1–18.

Chamkha, J. Ali. 2002. Hydromagnetic Combined convection flow in a vertical lid-driven cavity with internal heat generation or absorption. *Numerical Heat Transfer* 41: 529–546.

Chamkha, J. Ali, S. E. Ahmed. 2011. Unsteady MHD stagnation-point flow with heat and mass transfer for a three-dimensional porous body in the presence of heat generation/absorption and chemical reaction." *Journal of Applied Fluid Mechanics* 4(2): 87–94.

Chamkha, J. Ali, A. Al-Mudhaf. 2005. Unsteady Heat and mass transfer from a rotating vertical cone with a magnetic field and heat generation or absorption effects. *International Journal of Thermal Sciences* 44(3): 267–276.

Chamkha, J. Ali, A. F. Al-Mudhaf, I. Pop. 2006. Effect of heat generation or absorption on thermophoretic free convection boundary layer from a vertical flat plate embedded in a porous medium. *International Communications in Heat and Mass Transfer* 33(9): 1096–1102.

Choi, S. U. S. 1995. Enhancing thermal conductivity of fluids with nanoparticles. *ASME International Mechanical Engineering Congress & Exposition* MD-Vol.231: 99–105.

Hady, F. M., R. A. Mohamed, A. Mahdy. 2006. MHD free convection flow along a vertical wavy surface with heat generation or absorption effect. *International Communications in Heat and Mass Transfer* 33(10): 1253–1263.

Kasaeian, A., R. Daneshazarian, O. Mahian, L. Kolsi, A. J. Chamkha, S. Wongwises, I. Pop. 2017. Nanofluid flow and heat transfer in porous media: a review of the latest developments. *International Journal of Heat and Mass Transfer* 107: 778–791.

Kasim, A. R. M., N. F. Mohammad, S. Shafie. 2012. Effect of heat generation on free convection boundary layer flow of a viscoelastic fluid past a horizontal circular cylinder with constant surface heat flux. *AIP Conference Proceedings* 286(2012): 286–92. Khan, M.S. et al. 2014. Heat generation effects on unsteady mixed convection flow from a vertical porous plate with induced magnetic field. *Procedia Engineering*: 1–6.

Lin, Y., L. Zheng, X. Zhang. 2014. Radiation effects on marangoni convection flow and heat transfer in pseudo-plastic non-newtonian nanofluids with variable thermal conductivity. *International Journal of Heat and Mass Transfer* 77: 708–16.

Mahat, R., N. A. Rawi, A.R.M. Kasim, S. Shafie. 2017. mixed convection boundary layer flow of viscoelastic nanofluid past a horizontal circular cylinder : case of constant heat flux mixed convection boundary layer flow of viscoelastic nanofluid past a horizontal circular cylinder : Case of

constant heat flux. *Journal of Physics: Conference Series PAPER* 890.

Mahat, Rahimah, N. A. Rawi, A. R. M. Kasim, S. Shafie. 2018. Mixed Convection flow of viscoelastic nanofluid past a horizontal circular cylinder with viscous dissipation. *Sains Malaysiana* 47(7): 1617–1623.

Mamun, A. A., Z. R. Chowdhury, M. A. Azim, M. A. Maleque. 2008. Conjugate Heat transfer for a vertical flat plate with heat generation effect. *Nonlinear Analysis: Modelling and Control* 13(No.2): 213–223.

Merkin, J. H. 1977. Mixed convection from a horizontal circular cylinder. *International Journal of Heat and Mass Transfer* 20(1): 73–77. http://www.sciencedirect.com/science/article/pii/0017931077900862.

Nazar, R., N. Amin, I. Pop. 2002. Mixed convection boundary-layer flow from a horizontal circular cylinder in micropolar fluids: Case of constant wall temperature. *International Journal of Numerical Methods for Heat & Fluid Flow* 13(1): 86–109.

Nazar, R., L. Tham, I. Pop, D. B. Ingham. 2011. Mixed convection boundary layer flow from a horizontal circular cylinder embedded in a porous medium filled with a nanofluid. *Transport in Porous Media* 86(2): 517–36.

Olanrewaju, P. O., O. T. Arulogun, K. Adebimpe. 2012. Internal heat generation effect on thermal boundary layer with a convective surface boundary condition. *American Journal of Fluid Dynamics* 2(1): 1–4.

Rahman, A. R. M., M. A. Admon, S. Shafie. 2011. Free convection boundary layer flow of a viscoelastic fluid in the presence of heat generation. *World Academy of Science, Engineering and Technology* 5(3): 371–78.

Raju, M. C., N. A. Reddy, S. V. K. Varma. 2014. Analytical Study of MHD Free convective, dissipative boundary layer flow past a porous vertical surface in the presence of thermal radiation, chemical reaction and constant suction. *Ain Shams Engineering Journal* 5(4): 1361–1369.

Rashad, A. M., M. M. Rashidi, G. Lorenzini, S. E. Ahmed, A. M. Aly. 2017. Magnetic field and internal heat generation effects on the free convection in a rectangular cavity filled with a porous medium saturated with cu–water nanofluid. *International Journal of Heat and Mass Transfer* 104: 878–89.

Reddy, P. Sudarsana, A. J. Chamkha. 2016. Soret and dufour effects on MHD convective flow of Al_2O_3–water and TiO_2–water nanofluids past a stretching sheet in porous media with heat generation/absorption. *Advanced Powder Technology* 27(4): 1207–18.

Salleh, M. Z., R. Nazar, I. Pop. 2010. Mixed convection boundary layer flow over a horizontal circular cylinder with newtonian heating. *Heat and Mass Transfer* 46: 1411–1418.

Sheikholeslami, M., H. R. Ashorynejad, G. Domairry, I. Hashim. 2012. Flow and heat transfer of Cu-water nanofluid between a stretching sheet and a porous surface in a rotating system. *Journal of Applied Mathematics* 2012.

Sulochana, C., N. Sandeep. 2016. Stagnation Point Flow and Heat Transfer Behavior of Cu–water nanofluid towards horizontal and exponentially stretching / shrinking cylinders. *Applied Nanoscience*: 451–459.

Tham, L., R. Nazar, I. Pop. 2016. Mixed convection boundary layer flow from a horizontal circular cylinder in a nanofluid. *International Journal of Numerical Methods for Heat & Fluid Flow* 22(5): 576–606.

Tiwari, R. J., M. K. Das. 2007. Heat transfer augmentation in a two-sided lid-driven differentially heated square cavity utilizing nanofluids. *International Journal of Heat and Mass Transfer* 50(9–10): 2002–2018.

Ullah, I., K. Bhattacharyya, S. Shafie, I. Khan. 2016. Unsteady MHD mixed convection slip flow of casson fluid over nonlinearly stretching sheet embedded in a porous medium with chemical reaction, thermal radiation, heat generation/absorption and convective boundary conditions. *Plos One* 11(10): 1–35.

Vajravelu, K., A. Hadjinicolaou. 1993. Heat transfer in a viscous fluid over a stretching sheet with viscous dissipation and internal heat generation. *International Communications in Heat and Mass Transfer* 20: 417–30.

Zainuddin, N., I. Hashim, M. Ismoen, R. Roslan. 2015. The effect of radiation on free convection from a heated horizontal circular cylinder. *Applied Mechanics and Materials* 45(2015): 378–386.

Zainuddin, N., M. Ismoen, R. Roslan, I. Hashim. 2014. Oscillatory free convection about horizontal circular cylinder in presence of heat generation. *Mathematical Problems in Engineering* 658: 651–658.